Contact engineering for efficient charge injection in organic transistors with low-cost metal electrodes

D. Panigrahi, S. Kumar, and A. Dhar[a)]
Department of Physics, IIT Kharagpur, Kharagpur 721302, India

(Received 1 August 2017; accepted 6 October 2017; published online 23 October 2017)

Controlling charge injection at the metal-semiconductor interface is very crucial for organic electronic devices in general as it can significantly influence the overall device performance. Herein, we report a facile, yet efficient contact modification approach, to enhance the hole injection efficiency through the incorporation of a high vacuum deposited TPD [N,N′-Bis(3-methylphenyl)-N,N′-diphenylbenzidine] interlayer between the electrodes and the active semiconducting layer. The device performance parameters such as mobility and on/off ratio improved significantly after the inclusion of the TPD buffer layer, and more interestingly, the devices with cost effective Ag and Cu electrodes were able to exhibit a superior device performance than the typically used Au source-drain devices. We have also observed that this contact modification technique can be even more effective than commonly used metal oxide interface modifying layers. Our investigations demonstrate the efficacy of the TPD interlayer in effectively reducing the interfacial contact resistance through the modification of pentacene energy levels, which consequently results in the substantial improvement in the device performances. *Published by AIP Publishing.* https://doi.org/10.1063/1.4998603

In recent years, organic field effect transistors have attracted a significant amount of attention from the research community for their low production cost, ease of fabrication, and high mechanical flexibility with a huge variety of materials for fine-tuning the device properties. They have been widely utilized in many important applications, such as active-matrix displays, smart cards, smart sensors, radiofrequency identification tags, and complementary integrated circuits.[1–5] Among all the organic semiconductors, pentacene based transistors have emerged as strong potential candidates due to their superior electrical performance and device stability. Field effect mobility as high as 8.85 cm^2/V s and a high switching ratio of 10^7 have been achieved using pentacene as an active semiconducting layer, which is promising for its commercial exploitations.[6,7] In pentacene based field effect transistors, gold (Au) is commonly used as source-drain electrodes due to its inherently well matched work function ($W_f \sim 5.1$ eV) with the low lying HOMO level of pentacene, excellent electrical conductivity, and environmental durability.[6–8] Nevertheless, the high price of gold strongly limits its industrial applications and also inhibits its implementation in low cost electronic devices. To minimize the fabrication cost, comparatively low cost metal electrodes such as copper (Cu) and silver (Ag) have been considered as potential alternatives.[9,10] However, a relatively large contact resistance (R_c) for hole injection at the metal/semiconductor interface remains a major bottleneck for these inexpensive metals as their work functions ($W_f \sim 4.3$–4.7 for Ag and $W_f \sim 4.7$ eV for copper) do not match well with the pentacene HOMO level.[11,12] Furthermore, the direct contact between metal and pentacene can induce metallic mixture and dipoles at the interface, leading to a further increase in the barrier height by shifting the vacuum level alignments.[13] Therefore, contact engineering of the metal/semiconductor interface is very crucial to circumvent the above mentioned problems and hence, to achieve superior device performance without using gold source-drain electrodes. Several materials have been used in the past by many research groups to reduce interfacial contact resistance by tuning the interfacial properties.[14,15] Among them, metal oxides such as molybdenum oxide (MoO3) and vanadium pentoxide (V_2O_5) are commonly used as contact modifying buffer layers due to their large electron affinity and large work function.[16–18] However, the most critical issues of such metal oxides are their high sublimation temperature and poor compatibility with the delicate organic semiconductors. Organic materials can be severely degraded at high temperatures or under oxidizing atmosphere, which therefore seriously limits their application for the transistors with bottom gate top contact configurations.[19] In this work, we have employed an ultra-thin layer of TPD [N,N′-Bis(3-methylphenyl)-N,N′-diphenylbenzidine] deposited under high vacuum conditions between Ag electrodes and the pentacene channel layer in the top contact OFET devices to facilitate the hole injection from the metal to the semiconductor. The main motivation of using the TPD buffer layer was not only its well compatibility with pentacene, but also its low boiling point of 175 °C which does not degrade the performance of the active channel layer. Moreover, as TPD is soluble in most of the commonly used organic solvents, this contact modification technique can be beneficial for the transistors fabricated by means of the low cost wet deposition process. We have observed that after the incorporation of the TPD buffer layer, device performance parameters improved substantially and exhibited even better values than that of the devices with pristine Au metal electrodes. The reduction of contact resistance and therefore enhancement in interfacial charge injection efficiency in TPD modified devices are primarily accounted for such significant improvement in the device performance.

OFETs with the bottom gate top contact configuration were fabricated on glass substrates. The substrates were cleaned by sonication in sequential baths of acetone, propanol,

a)E-mail: adhar@phy.iitkgp.ernet.in

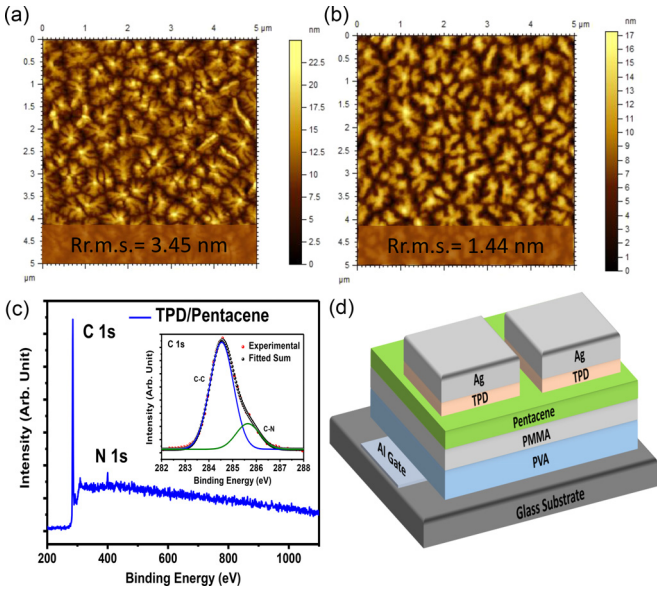

FIG. 1. (a) and (b) AFM topography images of pentacene and TPD/pentacene films, respectively. (c) XPS spectra of TPD/ pentacene thin films. (d) Schematic of the device structure with the TPD interface modifying layer.

and DI water for 20 min each and then dried by pure nitrogen gas. Nearly ~80 nm thick layer of aluminium was vacuum deposited on the clean glass substrates to form the gate electrodes for the OFET devices. A bilayer dielectric system of [poly(vinyl alcohol)] (PVA) and poly(methyl methacrylate) (PMMA) was deposited on the gate electrodes by the spin coating technique from their aqueous solution (60 mg/ml) and n-butyl acetate solution (60 mg/ml), respectively. The thickness of the bilayer dielectric film was estimated to be ~600 nm using Dektak profilometry measurements. Subsequently, a ~50 nm thick pentacene film was deposited under high vacuum conditions on top of the polymeric dielectric layer which served as the active semiconducting channel layer. Finally, Ag (~80 nm) source-drain electrodes were thermally deposited on top of the pentacene active layer to complete the OFET devices. The channel length and the width of the fabricated OFET devices were 50 μm and 2 mm, respectively. TPD and typical metal oxides (MoO_3 and V_2O_5) were thermally deposited prior to metallization through source-drain mask on top of the active semiconducting layer to modify the semiconductor/metal interface. The contact modifying layers were deposited with a pattern corresponding to that of the metal electrodes to rule out any possible charge transport from the source to drain electrode through the interlayers. The schematic of the fabricated OFET devices is shown in Fig. 1(d). Electrical measurements were performed using a Keithley 2450 programmable voltage–current source meter under dark conditions. Hole-only diodes were also fabricated to explore the charge injection mechanism in post-contact modification devices with the configurations Al/N,N′-Di(1-naphthyl)-N,N′-diphenyl-(1,1′-biphenyl)-4,4′-diamine (NPB) (60 nm)/pentacene (50 nm)/TPD (j nm)/Ag, where j = 0 and 4.

Prior to measuring the electrical performances of the transistors, AFM measurements were carried out to investigate any possible morphological changes occurring in pentacene after the deposition of the thin TPD layer. Figures 1(a) and 1(b) show the typical topological AFM images of pentacene and TPD/pentacene film grown on the PMMA dielectric layer. AFM images of pentacene showed a dendritic and terraced film morphology with closely packed structures. The r.m.s. surface roughness of the pentacene layer was obtained to be 3.45 nm, which is suitable for the uninterrupted transport of the charge carriers along the transistor channel. The deposition of the TPD interlayer reduces the roughness value to 1.44 nm, thereby improving the intimate contact with metal source and drain electrodes. In contrast, the deposition of metal oxide interlayers led to an undesirable increase in the rms roughness values (Fig. S2, supplementary material). It was also observed that after the conformal coating of the TPD layer, the dendritic crystalline structure of pentacene was well-maintained, which represents the efficacy of the TPD layer in preserving the original structure of the active channel layer (Fig. S3, supplementary material). X ray photoelectron spectroscopy was carried out to analyse the surface chemical composition as well as to evaluate the purity of the TPD deposited pentacene thin films. Wide-scan survey XPS spectra of the films as shown in Fig. 1(c) displayed two peaks at around 284.5 eV and 399.8 eV, which correspond to the presence of carbon and nitrogen, respectively.[20] The inset of Fig. 1(c) shows the deconvoluted C 1s XPS spectra of the TPD modified pentacene film. It exhibits two main components centered on 284.5 eV and 285.6 eV binding energy (B.E.) values which can be attributed to C-C and C-N groups, respectively.[21] The absence of any other impurity peak in the survey spectra demonstrates the purity of the deposited films, whereas the presence of the N1s peak confirmed the presence of TPD on the top of the pentacene surface.

Figure 2 shows the transfer and output characteristics of the OFET devices fabricated with various source and drain electrodes: pristine Ag, pristine Au, transition metal oxide (MoO_3 and V_2O_5) modified Ag electrodes, and TPD modified Ag electrodes. We have observed significant improvements in the pristine Ag device performance parameters after its interface modification through the TPD interlayer. The threshold voltage of the devices and the field effect mobility (μ) values of the charge carriers were calculated using the x-intercept and slope of the straight line in the plot of $I_d^{1/2}$ vs. V_g, respectively. Ag/TPD devices showed a reduced threshold voltage (V_{Th}) of −1.8 V, while the value was −7.7 V for pristine Ag devices. Smaller values of threshold voltage in the TPD modified Ag devices contribute to a reduction of contact resistance at a given gate voltage (V_G) by enhancing the effective gate bias $|V_G - V_{Th}|$.[22] Mobility values were found to increase drastically from 0.026 cm^2/V s to 0.09 cm^2/V s after metal-semiconductor interface modulation. We speculate that such remarkable improvement in the mobility values is due to the reduction of contact resistance at the silver/pentacene interface after its contact modification through TPD, which ensures better interfacial charge injection from Ag to pentacene. This improved hole injection in the TPD modified devices was also emulated in the enhanced on/off ratio of 10^4 in contrast to 10^3 in the pristine Ag devices. With the insertion of the TPD layer, the output current increased significantly to 3.8 μA which is almost 6 times higher than that of the devices without the TPD layer. We have estimated the values of subthreshold swing (SS) of the devices of both categories, i.e., with and without TPD

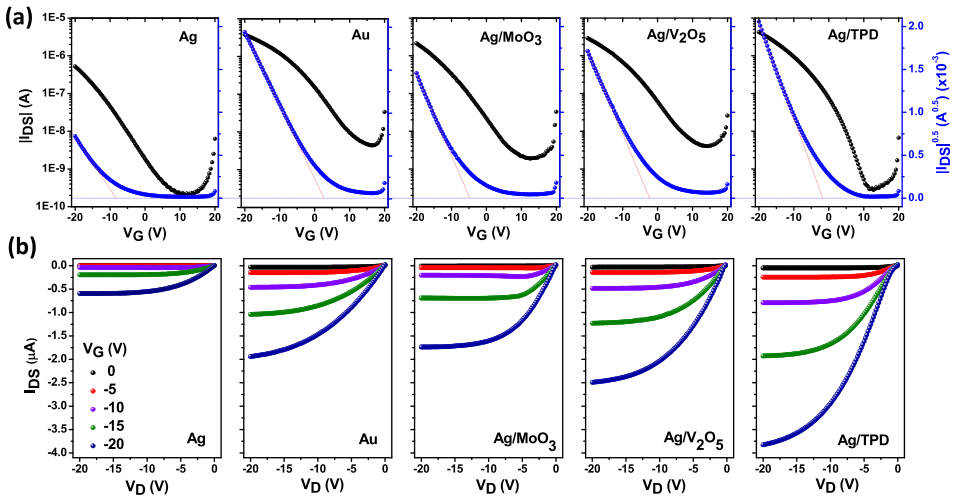

FIG. 2. (a) and (b) Transfer and output characteristics of the transistors with various electrodes: Ag, Au, Ag/MoO_3, Ag/V_2O_5, and Ag/TPD. V_G, V_D, and I_{DS} correspond to the gate voltage, drain voltage, and drain current, respectively.

modifications, and observed a reduction in the SS values from 8.6 V/decade to 3.8 V/decade after contact modifications. Lower values of SS indicate efficient collection of holes at the drain terminal and faster switching of drain current from the off to the on state. We have also observed that TPD modified Ag devices exhibited better performance than the devices with pristine Au and metal oxide modified Ag electrodes. The performance parameters of the transistors are summarized below in Table I which is representative of at least 10 devices for each category of the OFET devices. Before comparing the device performances, we have carefully optimized the thicknesses of various interface modifying layers to achieve the best possible outcome from the transistors (Fig. S1, supplementary material).

In order to unveil the effect of TPD contact modification on the hole injection mechanism, we have analysed the I-V characteristics of the fabricated diodes. In the diodes with only Ag electrodes, we observed 4 distinct injection mechanisms: (a) thermionic emission ($\ln I \propto V^{1/2}$) at very low voltage followed by (b) the ohmic regime ($I \propto V$) where conduction takes place through intrinsic thermally generated charge carriers, and current density depends not only on the applied voltage but also on the material conductivity, (c) space charge limited conduction (SCLC) regime where the voltage is high enough to initiate the injection of holes from Ag to pentacene along with the formation of space charges which limits the current according to the Mott-Gurney equation, $I \propto V^2$, and finally (d) trap filling limit (TFL) ($I \propto V^m$, $m > 2$) where all the available trap states are occupied by the injected holes, and as a result, current increases rapidly with the applied voltage.[23–25] The transition voltage (V_{TFL}) from SCLC to TFL was estimated to be 3.55 V in the case of pristine Ag devices. After the incorporation of the TPD interlayer, the whole I-V characteristics were fitted well by trap limited SCLC power law $I \propto V^m$ with higher values of m in the same applied voltage range. The value of V_{TFL} was also reduced to 1.9 V, which represents the efficacy of TPD in effectively reducing the contact resistance at the metal semiconductor interface and hence improving the charge injection from the metal to the semiconductor.[26] The measured I-V characteristics along with the fitting parameters of both the hole-only diodes are shown in Figs. 3(a) and 3(b). We have evaluated the reduction of contact resistance (R_c) at the silver/pentacene interface after the insertion of the TPD buffer layer by the Y function method (Fig. S4, supplementary material) and also compared the R_c values with Au/pentacene and transition metal oxide modified Ag/pentacene interfaces. This method is based on the straightforward analysis of the drain current (I_D) in the linear region ($V_D \ll V_G$) and considered to be a fast and precise way to estimate the values of Rc because only one transfer sweep is required for an individual transistor in contrast to the commonly used transfer-line method (TLM) with various channel lengths.[27,28] The values of R_c were found to decrease drastically from 0.7 MΩ cm in bare Ag electrodes to 0.05 MΩ cm after the addition of the TPD interlayer. A similar amount of improvement in contact resistance values was also observed using the transfer line method (Fig. S5, supplementary material). Apparently, such a large value of contact resistance and poor hole injection from the pristine silver electrode originate from the large hole injection barrier at the silver/pentacene interface. This energy barrier is effectively reduced after the incorporation of the TPD inter layer and results in a drastic improvement in the interfacial hole injection as well as overall device performance. Interestingly, it is also observed that TPD modified Ag devices exhibited lower values of contact resistance compared to pristine Au and metal oxide modified Ag devices [Fig. 3(c)]. To obtain deeper insight into the role of TPD in reducing the interfacial contact resistance, we have investigated the electronic energy levels of both pristine and TPD modified pentacene films by analysing their XPS valence band spectra. The relative position of the valence band maximum (VBM) with respect to the

TABLE I. Performance parameters of the transistors with various electrodes.

Electrodes	V_T (V)	I_{on}/I_{off}	μ_{sat} ($cm^2\,V^{-1}\,s^{-1}$)	I_{DS} (μA) ($V_G = V_D = -20V$)
Ag	-7.7 ± 0.6	$\sim 10^3$	0.026 ± 0.006	0.6
Cu	1.3 ± 0.7	$\sim 10^3$	0.04 ± 0.004	1.4
Au	2.8 ± 0.5	$\sim 10^3$	0.05 ± 0.005	1.9
Ag/MoO_3	-5.1 ± 0.6	$\sim 10^3$	0.065 ± 0.005	1.7
Ag/V_2O_5	-2.4 ± 0.4	$\sim 10^3$	0.066 ± 0.002	2.5
Ag/TPD	-1.8 ± 0.8	$\sim 10^4$	0.09 ± 0.01	3.8
Cu/TPD	2.1 ± 0.9	$\sim 10^3$	0.1 ± 0.01	5.0

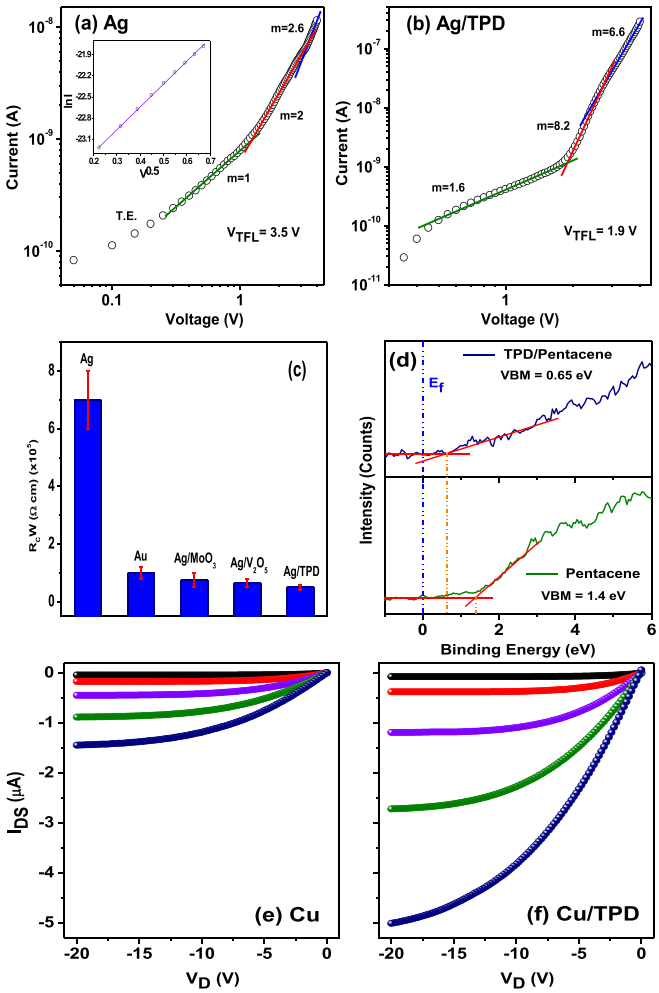

FIG. 3. (a) and (b) Double logarithmic representation of I-V characteristics of the hole-only diodes before and after TPD modification. Lines with different slopes represent different regimes of current conduction. (c) Contact resistance values of the transistors with various electrodes. (d) Valence band (VB) spectra of pristine and TPD modified pentacene obtained using the XPS technique. (e) and (f) Output characteristics of the transistors with Cu source/drain electrodes before and after interface modulation.

Fermi level (at zero binding energy) was estimated using extrapolation of linear fits of the initial edge of the XPS spectra with the base line [Fig. 3(d)]. The position of VBM (E_v) was observed to appear closer to the Fermi level (E_f) with $E_f - E_v = 0.65$ eV after the deposition of TPD while the difference was 1.4 eV in the case of the bare pentacene film which is consistent with the literature values.[29,30] As this response may arise from the pentacene/TPD interface and/or only TPD layer, we speculate that the shifting of the HOMO level is possibly due to the p-doping of pentacene. Such p-doping of pentacene can reduce the energy barrier for carrier injection by narrowing the depletion width at the interface and providing extra gap states to enhance the tunnelling probability of the injected carriers. It can also facilitate the charge transport by increasing the carrier concentration at the vicinity of the contacts.[31,32] Moreover, TPD can prevent the diffusion of metal atoms into pentacene and suppress the adverse effect of interface dipoles. These synergetic effects can explain the improvement in the device performance after the incorporation of the TPD layer. To further demonstrate the feasibility of this contact modification approach with other metal electrodes, we replaced Ag source/drain electrodes by Cu and fabricated the transistors with the same device architecture. Output characteristics of the devices are shown in Figs. 3(e) and 3(f) (corresponding transfer characteristics of the devices are shown in Fig. S6, supplementary material). Here also, we observed a significant amount of improvement in the overall device performance, consistent with the device performance enhancement in Ag source-drain devices. The charge carrier mobility increased to 0.1 cm^2/V s in contrast to 0.04 cm^2/V s in the case of pristine Cu devices. Such an improvement in mobility values was also emulated in the output characteristics of the devices. The output saturation current increased to 5 μA post contact modification with the TPD interlayer, which is almost four times that of the pristine Cu devices. We have also applied this contact modification technique on the high performance OFET devices ($\mu \sim 0.87$ cm^2/V s which was boosted up to 2.2 cm^2/V s after the incorporation of the TPD interlayer) and ensured its viability in effectively enhancing the charge injection at the metal-semiconductor interface (Fig. S7, supplementary material).

In summary, we have evaluated the feasibility of a high vacuum deposited, ultrathin TPD inter layer in effectively enhancing the charge injection efficiency from metal electrodes to the active semiconducting layer. The thermally evaporated TPD layer was found to be effective in the conformal covering of the underneath pentacene layer without causing any apparent damage, which demonstrates its compatibility with the delicate organic semiconductors. After the incorporation of the TPD layer, the contact resistance at the metal/semiconductor interface reduced substantially, thereby resulting in a remarkable improvement in the device performance. Our investigation demonstrated the efficacy of the TPD interlayer in improving the hole injection ability by forming the dominant trap limited SCLC conduction mechanism. Device analysis also exhibited that contact modification through the TPD interlayer can be much more effective than using pristine Au electrodes or interface modification through commonly used metal oxides. We therefore conclude that contact modification through the TPD buffer layer can be used as a low cost, convenient, and facile route to reduce the contact resistance at the metal/semiconductor interface and thus can be widely used in high performance OFET applications.

See supplementary material for the output characteristics of the pentacene/Ag transistors with interface modification through various thick metal oxide and TPD interlayers; AFM images of MoO_3/pentacene and V_2O_5/pentacene films; XRD pattern of pentacene and TPD/pentacene films; Variation of the Y function and $1/\sqrt{g_m}$ with the variation of V_G for the transistors with various electrodes; TLM measurement results of the transistors; Transfer characteristics of the transistors with Cu and Cu/TPD electrodes; and Device characteristics of the high performance transistors with Ag source/drain electrodes before and after interface modulation.

[1]H. Klauk, U. Zschieschang, J. Pflaum, and M. Halik, Nature **445**, 745 (2007).
[2]P. F. Baude, D. A. Ender, M. A. Haase, T. W. Kelley, D. V. Muyres, and S. D. Theiss, Appl. Phys. Lett. **82**, 3964 (2003).

[3]T. Someya, T. Sekitani, S. Iba, Y. Kato, H. Kawaguchi, and T. Sakurai, Proc. Natl. Acad. Sci. U. S. A. **101**, 9966 (2004).
[4]P. Lin and F. Yan, Adv. Mater. **24**, 34 (2012).
[5]J. T. Mabeck and G. G. Malliaras, Anal. Bioanal. Chem. **384**, 343 (2006).
[6]C.-Y. Wei, S.-H. Kuo, Y.-M. Hung, W.-C. Huang, F. Adriyanto, and Y.-H. Wang, IEEE Electron Device Lett. **32**, 90 (2011).
[7]X.-J. She, J. Liu, J.-Y. Zhang, X. Gao, and S.-D. Wang, Appl. Phys. Lett. **103**, 133303 (2013).
[8]S. W. Rhee and D. J. Yun, J. Mater. Chem. **18**, 5437 (2008).
[9]D. Ji, J. Jersch, and H. Fuchs, Adv. Electron. Mater. **2**, 1600215 (2016).
[10]X. Sun, Y. Liu, C. Di, Y. Wen, Y. Guo, L. Zhang, Y. Zhao, and G. Yu, Adv. Mater. **23**, 1009 (2011).
[11]S. Jeong, H. C. Song, W. W. Lee, H. J. Suk, S. S. Lee, T. Ahn, J.-W. Ka, Y. Choi, M. H. Yib, and B.-H. Ryu, J. Mater. Chem. **21**, 10619 (2011).
[12]T. Takahashi and T. Takenobu, Appl. Phys. Lett. **88**, 033505 (2006).
[13]N. J. Watkins, L. Yan, and Y. Gao, Appl. Phys. Lett. **80**, 4384 (2002).
[14]X. Yu, J. Yu, J. Zhou, J. Huang, and Y. Jiang, Appl. Phys. Lett. **99**, 063306 (2011).
[15]M. W. Alam, Z. Wang, S. Naka, and H. Okada, Appl. Phys. Lett. **102**, 061105 (2013).
[16]C. W. Chu, S. H. Li, C. W. Chen, V. Shrotriya, and Y. Yang, Appl. Phys. Lett. **87**, 193508 (2005).
[17]D. X. Long, Y. Xu, S. J. Kang, W. T. Park, E. Y. Choi, Y. C. Nah, C. Liu, and Y. Y. Noh, Org. Electron. **17**, 66 (2015).
[18]K. J. Baeg, G. T. Bae, and Y. Y. Noh, ACS Appl. Mater. Interfaces **5**, 5804 (2013).
[19]Y. Gao, Y. Shao, L. Yan, H. Li, Y. Su, H. Meng, and X. Wang, Adv. Funct. Mater. **26**, 4456 (2016).
[20]G. P. Mane, S. N. Talapaneni, C. Anand, S. Varghese, H. Iwai, Q. Ji, K. Ariga, T. Mori, and A. Vinu, Adv. Funct. Mater. **22**, 3596 (2012).
[21]X. Yang, J. Li, J. Liu, Y. Tian, B. Li, K. Cao, S. Liu, M. Hou, S. Li, and L. Ma, J. Mater. Chem. A **2**, 1550 (2014).
[22]S. Choi, C. Fuentes-Hernandez, C. Y. Wang, T. M. Khan, F. A. Larrain, Y. Zhang, S. Barlow, S. R. Marder, and B. Kippelen, ACS Appl. Mater. Interfaces **8**, 24744 (2016).
[23]Z. Chiguvare and V. Dyakonov, Phys. Rev. B **70**, 235207 (2004).
[24]T. P. Nguyen, P. Girault, C. Renaud, F. Reisdorffer, P. Le Rendu, and L. Wang, J. Appl. Phys. **115**, 012013 (2014).
[25]K. Fukuda and N. Asakawa, J. Phys. D: Appl. Phys. **50**, 055102 (2017).
[26]W. Wang, J. Han, J. Ying, and W. Xie, IEEE Trans. Electron Devices **61**, 3507 (2014).
[27]H. Y. Chang, W. Zhu, and D. Akinwande, Appl. Phys. Lett. **104**, 113504 (2014).
[28]Y. Xu, T. Minari, K. Tsukagoshi, J. A. Chroboczek, and G. Ghibaudo, J. Appl. Phys. **107**, 114507 (2010).
[29]B. Lüssem, M. L. Tietze, H. Kleemann, C. Hoßbach, J. W. Bartha, A. Zakhidov, and K. Leo, Nat. Commun. **4**, 2775 (2013).
[30]H. S. Kim, H. Lee, P. E. Jeon, K. Jeong, J. H. Lee, and Y. Yi, J. Appl. Phys. **108**, 53701 (2010).
[31]T. Minari, P. Darmawan, C. Liu, Y. Li, Y. Xu, and K. Tsukagoshi, Appl. Phys. Lett. **100**, 093303 (2012).
[32]D. X. Long, Y. Xu, H. X. Wei, C. Liu, and Y. Y. Noh, Phys. Chem. Chem. Phys. **17**, 20160 (2015).